Magnetic field measurements on moderately active cool dwarfs[*]

I. Rüedi[1], S.K. Solanki[1], G. Mathys[2], and S.H. Saar[3]

[1] Institute of Astronomy, ETH–Zentrum, CH–8092 Zürich, Switzerland
[2] European Southern Observatory, Casilla 19001, Santiago 19, Chile
[3] Center for Astrophysics, 60 Garden Street, Cambridge, MA 02138, USA

Abstract. We present a careful analysis of 13 high-quality optical spectra of low to moderately active late-type dwarfs (G1-K5) aimed at determining their magnetic parameters. Among our sample only one star, ϵ Eri (spatially averaged field strength $\approx 165 \pm 30$ G), exhibits the unambiguous signature of a magnetic field, a few are candidates and the remaining show no sign of a magnetic field in the observed spectra. Our analysis is based on an inversion of the spectra using detailed numerical solutions of the Unno-Rachkovsky equations, for multiple spectral lines at different positions on the stellar disk, and including magneto-optical effects. It gives results for ϵ Eri which are in good agreement with the detailed analysis of infrared spectra by Valenti et al. (1995). However, the low value of the spatially averaged field strength of these recent analyses imply that most values of the magnetic flux determined previously for moderately active stars are probably too large, often by considerable amounts. We find that the magnetic flux can be reliably determined if considerable care is taken in the analysis, but the magnetic field strength and filling factor cannot be determined separately for moderately active stars with optical spectra of spectral resolution $\leq 10^5$ and S/N ≤ 250.

In the case of ϵ Eri we are able to constrain the temperature of the detected magnetic features, which we find to be similar to or hotter than the non-magnetic surroundings, providing the first direct evidence that the detected field is in the form of plages. We also find that if an inversion approach is used, which determines various line broadening parameters simultaneously in a self-consistent manner, the presence of a magnetic field is not as obvious as some previous analyses have suggested. In addition, we determine fundamental parameters of the stellar sample.

Key words: stars: magnetic fields – stars: activity – stars: late-type – stars: fundamental parameters

Send offprint requests to: I. Rüedi

1. Introduction

Magnetic fields are responsible for a great variety of active phenomena on the sun and other solar-like stars. Precise magnetic field measurements of solar-like stars would enable us to better constrain dynamo theories, as well as models of chromospheric and coronal heating.

Various methods have been used for measuring magnetic fields on cool stars. Early methods relied on a Fourier analysis of a spectral line pair (Robinson 1980, Robinson et al. 1980) or of a larger number of spectral lines (Gray 1984a). Others are based on more or less sophisticated radiative transfer calculations, most of the time also applied only to one spectral line pair (e.g. Marcy 1984, Basri & Marcy 1988 and Marcy & Basri 1989), although individual analyses are based on a corresponding multi-line analysis (e.g. Saar et al. 1986, Basri et al. 1992, Valenti et al. 1995). Mathys & Solanki (1989) followed another approach: they used the Stenflo & Lindegren (1977) method, a statistical analysis of a large number of spectral lines based on line width measurements at different levels in the line profile in order to reduce the effects of small, hidden blends. Queloz et al. (1996) also applied a statistical analysis to their data set. On stars with large $v \sin i$, the Stokes V, i.e. net circularly polarized, signal can be detected (Donati et al. 1990, 1992a, 1992b), while for active K and M stars lines at 2.2 μm allow direct measurements of the magnetic field (Saar & Linsky 1985; Saar 1996). For reviews of the subject see Saar (1990, 1994) and Solanki (1992).

In this paper we present a detailed report of a new multi-line analysis, more precisely an inversion, of optical spectra based on sophisticated radiative transfer calculations. In order to carry out a consistent magnetic field analysis, we first determine the fundamental parameters of the stars in our sample using the same inversion code and models.

The structure of the paper is as follows: We first describe the observations in Sect. 2 and, in Sect. 3, the method of analysis as well as the models used. Then, in Sect. 4, we present the first part of the data analysis, i.e. the determination of the fundamental stellar parameters. We next carry out a number of tests concerning magnetic field determination on the most stud-

Table 1. Journal of observations

Name	HR	Date	Detector
58 Eri	1532	24 Jan 1989	CCD
α Cen A	5459	4 May 1988	RETICON
	2667	22 Jan 1989	CCD
	3538	24 Jan 1989	CCD
	4979	1 May 1988	RETICON
61 Vir	5019	3 May 1988	RETICON
τ Ceti	509	15 Oct 1986	RETICON
40 Eri A	1325	20 Oct 1986	RETICON
α Cen B	5460	4 May 1988	RETICON
36 Oph B	6401	3 Mai 1988	RETICON
ϵ Eri	1084	19 Oct 1986	RETICON
	5568	2 Mai 1988	RETICON
ϵ Indi	8387	11 Oct 1987	RETICON

ied late-type star in our sample, ϵ Eri. These are described and compared with previous results in Sect. 5. Sect. 6 deals with the magnetic results obtained for 13 late-type stars (G1-K5) and, finally, Sect. 7 contains our conclusions.

2. Observations and stellar properties

2.1. The observations

Thirteen relatively bright late-type stars were observed with the 1.4 m Coudé Auxiliary Telescope (CAT) of the European Southern Observatory and the Coudé Echelle Spectrograph (CES). The data were collected during four runs: in October 1986, October 1987, May 1988 and January 1989. The detailed journal of the observations is given in Table 1.

The long camera of the CES was used for all observations with either a RETICON or (in 1989 only) a CCD (RCA, referred to internally at ESO as #9) as a detector. Both detectors have a pixel size of 15 μm (in the dispersion direction for the RETICON – the CCD has square pixels). The slit width was adjusted so as to achieve a resolving power of 10^5 in all cases (corresponding to a projected FWHM of approx. 2.4 px on the detector). The S/N ratio varies somewhat from one star to the next, but is always at least 250.

Several spectra were taken for each star, at different central wavelengths (in different orders of the CES). As a result, large wavelength ranges were observed. For instance, for α Cen A and α Cen B the spectra cover the range $5380.4 - 8734.1$Å with few interruptions, mainly corresponding to absorption bands of the earth atmosphere. For other stars smaller, but still considerable wavelength regions were recorded. They were chosen to contain a sufficient number of lines of interest for magnetic field measurements. Note that all the exposures of a given star were always obtained on a single night in order to ensure that all parts of the observed spectrum refer to practically the same rotational phase of the star. Also, care was taken to observe the various ranges "randomly" (as opposed to in order of increasing or decreasing wavelength), so as to avoid that possible time variations might be mistaken for wavelength dependences. The following 4 wavelength ranges are

analysed here: 6077.5–6104.7 Å, 6131.3–6158.7 Å, 6231.0–6259.2 Å and 6832.8–6863.0 Å for the CCD spectra, or 6059.7–6110.4 Å, 6142.8–6191.1 Å, 6202.7–6255.5 Å and 6817.3–6873.6 Å for the RETICON spectra.

Data reduction was performed as follows. First bias (obtained in independent exposures) and dark current were subtracted. For the RETICON, the dark current was interpolated between the masked pixels at both ends of the spectrum (see Mathys & Solanki 1989 for more details). For the CCD, it was instead evaluated from the regions of the frame on both sides of the spectrum in the spatial direction. In the latter case, in fact, not only the dark current is removed in this way, but also the sky background and any possible scattered or parasitic light in the spectrograph. These contributions cannot be taken into account for the RETICON, but given the brightness of the star observed, we estimate that they should be mostly negligible: consideration of our CCD spectra as well as our experience with the instrumentation suggest that they are unlikely to exceed 0.1% of the continuum level.

In the next step, the stellar exposures were flat-fielded by dividing them by the average of a series of spectra of a white lamp internal to the spectrograph (taken in the same conditions), to correct them from pixel-to-pixel variations of the detector sensitivity and, in the case of the CCD, from optical interference fringes originating as a result of back illumination through the thinned substrate. In spite of this, some slight residual fringes are left in some of the redder portions of the CCD spectra, but they should not exceed 0.3% of the continuum level. As a result, the S/N ratio achieved after reduction varies somewhat from one star to the next, but is always at least 250.

Continuum normalization was carried out by fitting a low-degree polynomial to the highest points of the spectra. For the CCD spectra 3rd order polynomials were used, while 5th, or in some cases 6th, order polynomials were used for the RETICON spectra due to their larger wavelength coverage. By comparison with the solar spectrum we estimate the position of the continuum to be accurate to always better than 1% and in most cases even to 0.2%.

The wavelength calibration was performed internally using the stellar lines themselves. Their positions in the stellar spectra were determined by fitting Gaussians to them. The wavelength (pixel-fractions) of their centre were then identified with the values listed in the KPNO table of solar wavelengths (Pierce & Breckinridge 1973). A second-degree (for the CCD spectra) or third-degree (for the RETICON spectra) polynomial fit was computed for the wavelength-pixel relation. Depending on the spectrum 10 to 40 lines were used for the calibration. The standard deviation of the measured wavelength about the best-fit polynomial ranges from 0.05 to 0.12 pixel which corresponds to 1.4 to 3.3 mÅ.

2.2. The stars

All the observed stars are fairly bright, moderately active or inactive G and K main-sequence stars that are either single or parts

of well separated binary systems. There follow a few comments on each star. The stars are listed in order by spectral type.

58 Eri (HR 1532) is an active G1 dwarf ($F_X \approx 15 F_X(\odot)$, where $F_X(\odot) = 6.3 \cdot 10^4$ ergs cm^{-2} s^{-1} is the solar value of the X-ray flux (Schrijver 1983); Hempelmann et al. 1995) with strong Li I absorption (Pasquini et al. 1994), probably indicating youth. Based on Ca II H and K modulation $P_{rot} = 10.8$ days (Donahue, priv. comm.) where P_{rot} is the rotation period. The star shows only chaotic long-term Ca II variations (Baliunas et al. 1995). Saar & Osten (1996), studying seven lines between 6150 Å and 6180 Å, find a weak trend in velocity broadening with the effective Landé factor g_{eff}, suggesting the possible presence of significant magnetic flux. No actual magnetic measurements, however, exist for this star.

α Cen A (HR 5459), our stellar neighbor, is an inactive ($F_X \approx 0.3 F_X(\odot)$; Hempelmann et al. 1995) G2 dwarf about 5–6 Gyr old (Noels et al. 1991). Hallam et al. (1991) determined $P_{rot} \approx 29$ days, based on modulation of ultraviolet emission lines. Saar & Osten (1996) obtain no evidence for magnetic broadening.

HR 2667 is a G3 dwarf with Ca II flux less than the Sun's (Pasquini 1992). It is part of a common proper motion triplet with HD 53706 (K0V) and a fainter K2 dwarf. No previous high resolution measurement of its velocity broadening parameters or its magnetic field has been made to our knowledge.

HR 3538 is a moderately active G3 dwarf ($F_X \approx 5 F_X(\odot)$; Hempelmann et al. 1996) with an estimated $P_{rot} \approx 15.0$ days (Noyes et al. 1984). It shows a weak 2.5 year cycle in the 25 year Mount Wilson Ca II time series (Baliunas et al. 1995). Marcy (1984) detects a magnetic field, but Saar & Osten (1996) find no evidence for a field.

HR 4979 is a G3 dwarf with unusually strong Li I absorption (Soderblom 1985). While this can imply youth, its low $v \sin i$ value and low levels of activity (Pasquini & Pallavicini 1991) suggest that, instead, HR 4979 may have anomalous Li I, like some other old stars (e.g. Duncan 1981). The star's unusually broad Hα line (Pasquini & Pallavicini 1991) and our log g value support the idea that the star is older and somewhat evolved (g is the gravitational acceleration). Ayres et al. (1995) find $F_X = 1.9 F_X(\odot)$. Saar & Osten (1996) find no evidence for magnetic broadening.

61 Vir (HR 5019) is an old, inactive ($F_X \leq 0.4 F_X(\odot)$; Ayres et al. 1995) G6 dwarf. The rotational period from Ca II modulation is 32.7 days (Noyes et al. 1984). The star has been monitored only since 1977 at Mount Wilson, and shows variable Ca II emission with as yet no clear cyclic signature (Baliunas et al. 1995). Gray (1984a, b) analyzed spectra both with and without invoking magnetic fields. He obtained a preliminary detection of a magnetic field.

τ Ceti (HR 509) is an inactive ($F_X = 0.25 F_X(\odot)$; Hempelmann et al. 1996) G8 dwarf with very weak Li I (e.g., Rebolo et al. 1986), suggesting considerable age. The star shows essentially non-variable long-term Ca II behavior (Baliunas et al. 1995), though Gray & Baliunas (1994) suggest that a weak, low amplitude 11 year cycle may be present. The empirical Ca II - rotation relation predicts a rotation period of $P_{rot} = 31.9$ d (Noyes

et al. 1984). Gray's (1984a) uncertain magnetic field detection is probably spurious; no other magnetic analysis has shown evidence for a field (Marcy 1984; Mathys & Solanki 1989) and no trend is seen between line broadening and g_{eff} by Saar & Osten (1996).

40 Eri A (HR 1325) is an old K1 dwarf in a triple system with a DA white dwarf and an M4.5V dwarf. The rotation period estimated from the mean Ca II H and K level is $P_{rot} = 37.0$ days (Noyes et al. 1984). The star shows a strong cyclic Ca II variation with a 10.1 year period (Baliunas et al. 1995). Ayres et al. (1995) find $F_X = 1.1 F_X(\odot)$. Valenti et al. (1995) analyze high resolution infrared spectra and set an upper limit on the magnetic field of $B = 1710$ G and on the magnetic filling factor $\alpha = 2.7\%$. The upper limits on the magnetic filling factor α and the magnetic field strength B are consistent with non-detections by Saar (1988) and by Saar & Osten (1996).

α Cen B (HR 5460), is α Cen A's companion - an inactive ($F_X \approx 0.6 F_X(\odot)$; Hempelmann et al. 1995) K1 dwarf about 5–6 Gyr old, like α Cen A (Noels et al. 1991). Char et al. (1993) find $P_{rot} \approx 43$ days based on modulation of Ca II HK core emission, consistent with the P_{rot} expected from rotation–activity relations. Saar & Osten (1996) failed to detect any sign of magnetic broadening.

36 Oph B (HR 6401) is a moderately active K1 dwarf ($F_X \sim$ 60% of ϵ Eri; Hempelmann et al. 1995), part of a triple system with 36 Oph A (K1V) and HD 156026 (K5V). Its rotational period is well determined at $P_{rot} = 21.1$ days (Donahue et al. 1996). The star shows a cyclic Ca II variation with a 5.7 year period, though considerable chaotic variability is superimposed (Baliunas et al. 1995). Marcy (1984) claimed a magnetic field detection, but Saar & Osten (1996) find no evidence for significant magnetic broadening.

ϵ Eri (HR 1084) is an active K2 dwarf with strong Ca II emission, a rotational period of $P_{rot} = 11.68$ days (Donahue et al. 1996), and photometric evidence for spot coverage of a few percent of the stellar surface (e.g., Frey et al. 1991). The star's Ca II emission shows primarily chaotic long-term variability - no *clear* cyclic behavior is present (Baliunas et al. 1995; however, see Gray & Baliunas 1995, who claim a possible weak, underlying 5 year cycle). Its X-ray surface flux is about 10 times that of the Sun (e.g., Schrijver 1983). Smith (1983) noted excess broadening in some higher g_{eff} Mn I lines and attributed it to magnetic fields (although in retrospect it could also have been due to hyperfine splitting). Gray (1984a, b) followed with a measurement of $v \sin i \approx 2.2$ km s^{-1} and $v_{mac} \approx 2.4$ km s^{-1} if $\alpha B \equiv 0$, and $v \sin i \approx 2.1$ km s^{-1} and $v_{mac} \approx 1.0$ km s^{-1} if $B \sim 1900$ G and $\alpha \sim 0.3$ (v_{mac} is the macroturbulence velocity). Several other magnetic field measurements have been reported (Marcy 1984; Saar et al. 1986; Basri & Marcy 1988; Saar 1988; Mathys & Solanki 1989; Valenti et al. 1995) and are discussed in detail by Saar (1990) and Valenti et al. (1995). The most reliable measurement (Valenti et al. 1995), based on detailed radiative transfer modeling of several high resolution ($\lambda/\Delta\lambda = 10^5$), high S/N ($\sim$ 100) infrared lines found $\alpha = 8.8\%$ and $B = 1440$ G, considerably less than almost all previous measurements (excepting Saar 1988).

Table 2. Stellar parameters from the literature

Name	HR	HD	Spectral Type	T_{eff} [K]	$\log g$	$\log[\mathrm{Fe/H}]$	$v \sin i$ [km s^{-1}]	v_{mac} [km s^{-1}]
58 Eri	1532	30495	G1V	5787 – 6000	4.50 – 4.71	0.10 – 0.25	1.6–4.3	1.7–4.8
α Cen A	5459	128620	G2V	5720 – 5800	4.14 – 4.35	0.10 – 0.22	1.8–2.7	2.8
	2667	53705	G3V	5870	4.30	−0.25	–	–
	3538	76151	G3V	5684 – 5810	4.50 – 4.55	0.07 – 0.28	0.9–1.6	2.8–3.3
	4979	114613	G3V	5600 – 5700	≤ 4.50	0.20	2.7	2.7
61 Vir	5019	115617	G6V	5570 – 5684	4.00 – 4.51	−0.03 – 0.20	0.0–2.0	2.5–3.6
τ Ceti	509	10700	G8V	5250 – 5529	4.50 – 4.60	−0.28 – −0.38	0.1–0.9	1.0–2.6
40 Eri A	1325	26965	K1V	5072 – 5230	4.31 – 4.49	−0.34 – −0.14	1.0–1.4	1.4–2.4
α Cen B	5460	128621	K1V	5200 – 5325	4.58 – 4.63	0.26	1.1–3.0	1.0
36 Oph B	6401	155885	K1V	5090 – 5165	4.49 – 4.60	−0.30 – −0.14	1.1–1.4	1.3–2.4
ϵ Eri	1084	22049	K2V	4990 – 5203	4.71 – 4.80	−0.20 – 0.17	1.0–2.2	1.0–3.0
	5568	131977	K4V	4625 – 4690	4.79	0.01	0.7–2.0	1.2
ϵ Indi	8387	209100	K5V	4580	4.50	−0.23	0.7	0.6

HR 5568 is a low activity K4 dwarf ($F_X < 0.6F_X(\odot)$; Wood et al. 1994) with an M2 (HD 131976) companion in a hyperbolic orbit. Basri & Marcy (1994) find no evidence for a magnetic field (suggesting Marcy's 1984 measurement was probably spurious); Saar & Osten (1996) concur.

ϵ Indi (HR 8387) is the title member of an old moving group, and has activity levels consistent with this age ($F_X = 1.6F_X(\odot)$; Ayres et al. 1995).

Table 2 summarizes the literature values of the main parameters of these stars, listed according to spectral type. The first column gives the common name of the star. The second and third column contains their HR and HD identification numbers, while the fourth column lists the spectral type. The effective temperature, T_{eff}, the gravitational acceleration, g, the logarithmic iron abundance relative to that of the sun, $\log(\mathrm{Fe/H})$, the rotational velocity, $v \sin i$, and the macroturbulence, v_{mac}, are listed in column 5, 6, 7, 8 and 9, respectively. The sources of the tabulated data are listed below.

HR 1532: Gehren (1981), Valenti (1994), Saar & Osten (1996)

HR 5459: Dravins & Nordlund (1990), Cayrel de Strobel et al. (1992), Chmielewski et al. (1992), Anderson & Edvardsson (1994), Taylor (1994), Saar & Osten (1996)

HR 2667: Chmielewski et al. (1991)

HR 3538: Cayrel de Strobel & Bentolila (1989), Gray & Johanson (1991), Taylor (1994), Valenti (1994), Saar & Osten (1996)

HR 4979: Soderblom (1985), Pasquini & Pallavicini (1991), Randich et al. (1993), Saar & Osten (1996)

HR 5019: Gray (1984a, b, 1994), Bell et al. (1985), Perrin et al. (1988), Gray & Johanson (1991), Taylor (1994), Valenti (1994)

HR 509: Gray & Johanson (1991), Gray (1984b), Cayrel de Strobel et al. (1992), Blackwell & Lynas-Gray (1994), Gray (1994), Gray & Baliunas (1994), Taylor (1994), Valenti (1994)

HR 1325: Steenbock (1983), Blackwell & Lynas-Gray (1994), Taylor (1994), Valenti (1994), Saar & Osten (1996)

HR 5460: Dravins & Nordlund (1990), Cayrel de Strobel et al. (1992), Chmielewski et al. (1992), Hale (1994), Taylor (1994), Saar & Osten (1996)

HR 6401: Cayrel de Strobel et al. (1992), Taylor (1994), Valenti (1994), Saar & Osten (1996)

HR 1084: Smith (1983), Gray (1984a, b), Abia et al. (1988), Marcy & Basri (1989), Gray & Johanson (1991), Gray (1994), Taylor (1994), Valenti (1994), Saar & Osten (1996)

HR 5568: Hearnshaw (1976), Hale (1994), Taylor (1994), Saar & Osten (1996)

HR 8387: Abia et al. (1988), Saar & Osten (1996)

3. Method of analysis

The data were fitted using the inversion code introduced by Solanki et al. (1992, 1994). It is based on an automated Levenberg-Marquardt least-squares fitting procedure during which the free parameters of the model are varied until the sum of the squared differences between the observed spectrum and the synthetic line profiles reaches a minimum. The synthetic line profiles result from LTE radiative transfer calculations (based on the Diagonal Element Lambda Operator, DELO, technique of Rees et al. 1989, including magnetooptical effects, the complete Zeeman pattern, etc.) in a two-component atmospheric model. The first component is field free, while the second is permeated by a height-independent magnetic field, B, covering a fraction α (the magnetic filling factor) of the stellar surface. The magnetic component was assumed to be evenly spread over the stellar surface, although this is obviously not always the case, as can be seen on the sun, where the active regions are concentrated near the equator. [1] The sun does have a considerable portion of its flux in the much more homogeneously distributed magnetic network, however. Also, without more detailed knowledge of the true distribution of the field at the time of the observation, the assumption of homogeneity is the best one can make. We further assume that the magnetic field points in the direction

---

[1] Doppler-imaged stellar surfaces show large polar spots on, e.g., rapidly rotating RS CVn primaries (e.g., Vogt & Penrod 1983, Strassmeier et al. 1991), but these stars are in general so much more active than the stars we consider here that the two cannot be directly compared.

of the stellar radius, i.e. that it is always vertical relative to the local stellar surface. The above assumptions are standard for stellar magnetic field measurements. One of the improvements of the present analysis compared to older ones is the possibility of using an atmospheric model for the magnetic component that is different from that of the surrounding field-free atmosphere.

The atmospheric models used in this work are based on those of Kurucz (1991). Unless specified, the fits were carried out using the same atmospheric model for both (magnetic and non-magnetic) components. In some cases, the temperature of the magnetic region was allowed to vary while the temperature of the non-magnetic component was kept fixed at the value determined from the preanalysis of the spectra using the same data set, inversion code and atmospheric models (cf. Sect. 4).

To generate the stellar flux profile, we must compute the intensity profile at a number of μ values (n_μ) and sum these $I(\mu)$ (with appropriate Doppler shifts) over the stellar disk. The most efficient method of disk-integration for the purpose of velocity broadening measurements (when $B = 0$) is to divide the disk into azimuthal sectors of equal projected area (see Bruning 1984). This method is less efficient for magnetically split lines however (due to their different center-to-limb behavior), and requires more sectors for equal accuracy. Since we are interested in modeling stars which both rotate and may have measurable magnetic fields, and since the analysis we are using is computationally voracious, a compromise is needed.

To achieve the most accurate disk-integration with a minimal n_μ, we have used a set of five "optimum" μ values of the type tabulated by Saar et al. (in prep.). In this formulation, equal projected area sectors (centered at μ) are used in the disk integration, but the intensity assigned as the proper "average" profile for each sector is adjusted to values $I(\mu')$. These μ' values have been computed to optimize accurate reproduction of a magnetic flux profile with $n_\mu = 100$. In this paper, we used a slightly less refined set of "optimum" μ' values than those given by Saar et al. (in prep.); differences in the results, however, should be slight.

The microturbulent velocity broadening was modelled, as is usually done, by a Gaussian. The profile shapes best suited to model the macroturbulence and in particular the instrumental broadening are less certain. We tried different combinations: the instrumental broadening was modelled either by a Gaussian or exponential function, while the macroturbulent broadening was modelled by a Gaussian or the radial-tangential velocity broadening function (Gray 1988). The main problem is the unknown instrumental profile shape. We find that the χ^2 of the fits is of equal quality for either profile shape. However, the derived value of the macroturbulence is extremely sensitive to the chosen instrumental profile form, being up to a factor of 4 smaller if the exponential profile is used instead of the Gaussian. Furthermore, we find that the χ^2 decreases substantially if we choose an instrumental profile less broad than it nominally would be for a resolving power of 100 000, while letting the radial-tangential macroturbulence absorb a part of the instrumental contribution (obviously the instrumental profile shape is closer to a radial-tangential profile than to the other profile forms, but it is not

clear to us how spectral resolving power relates to the width of the radial-tangential function). We obtained the best results by taking a Gaussian of width 1.0 km s^{-1} to represent a part of the instrumental broadening. The remaining part, as well as the macroturbulence are contained in a radial-tangential velocity broadening function whose width is a free parameter of the fit. This is the approach we finally adopted for all the fits. Therefore the macroturbulence values obtained in our analysis are unreliable. Finally, it should be noted that the values of the rotational velocity we obtained may well depend on the choice of profile of the macroturbulence and instrumental profile.

The spectral lines used in this work are listed in Table 3. In order to avoid inconsistencies due to differences between the relative abundances of different elements from star to star, we restricted ourselves to the use of iron lines only. The ion is given in the first column and the wavelength of the transitions in the second column. Column 3 lists the effective Landé factor of the transitions as computed from LS-coupling, g_{eff}. We used the LS-coupling values since they do not differ from the empirical values by more than 2%. Columns 4 and 5 list the excitation energy of the lower atomic level, χ_e, and, $\delta\Gamma_6$, the fudge factor to the van der Waals damping constant, respectively. $\delta\Gamma_6$ was set to a fixed value for each line separately. These values were taken from the literature, when available (Simmons & Blackwell 1982) or extrapolated therefrom with the additional condition that $\delta\Gamma_6 \leq 2.5$ (cf. Solanki 1987). The good fits to the solar profiles resulting from this procedure justified it. Finally, the logarithmic oscillator strengths, $\log gf$, derived by Thévenin (1990) and by us (in Sect. 4.1) are tabulated in columns 6 and 7.

For the determination of the fundamental stellar parameters in Sect. 4.2, the $\log gf$ values were treated as fixed parameters, so that the Fe abundance values of each star could be determined in a consistent manner. The $\log gf$ values which we used for this purpose were determined from a fit to the integrated solar flux spectrum of Neckel (1994) with the same inversion code and models. These solar fits are described in Sect. 4.1.

Later, for the magnetic analysis (Sects. 5 & 6), we treated the $\log gf$ values as free parameters, following Basri & Marcy (1988), who had argued that the use of solar $\log gf$ values is inappropriate for the magnetic analysis of different stellar types. As a consequence, the abundance values determined in Sect. 4.2 were used as fixed parameters while the $\log gf$ values were allowed to vary for the "magnetic" analysis. The strength of each line (parameterized here by its $\log gf$ value) reacts differently to differences between the thermodynamic structures of the magnetic and non-magnetic areas, whereas the abundance should not be different in the two components. Also, due to the minuteness of the magnetic influence on the line profiles, it is important to have very good fits to the observed profiles. Small differences in, e.g. the temperature gradient from star to star (due to abundance differences, convection, gravitational acceleration or magnetic activity) lead to differences between observed and synthetic profiles. Allowing the $\log gf$ values of the lines to be variable during this stage of the analysis is a simple way of compensating for such unknowns.

Table 3. Lines used

Ion	λ [Å]	g_{eff}	χ_e [eV]	$\delta\Gamma_6$	$\log gf$ Thévenin	$\log gf$ This work
Fe I	6082.7	2.0	2.22	1.2	−3.68	−3.50
Fe I	6151.6	1.83	2.18	1.3	−3.40	−3.23
Fe I	6173.3	2.5	2.22	1.3	−2.98	−2.80
Fe I	6240.6	1.0	2.22	1.2	−3.41	−3.22
Fe I	6820.3	1.5	4.64	2.5	−1.27	−1.13
Fe I	6842.6	2.5	4.64	2.5	−1.28	−1.15
Fe I	6843.6	1.125	4.55	2.5	−0.98	−0.85
Fe I	6857.2	1.125	4.07	2.4	−2.21	−2.05
Fe II	6149.3	1.33	3.89	2.5	−2.88	−2.85
Fe II	6247.6	1.1	3.89	2.5	−2.55	−2.48

Our set of lines includes both, lines having large ($g > 2$) and lines with small Landé factors, in order to differentiate between Zeeman broadening and other sources of line broadening (rotation, turbulent velocity, instrument, etc.). The selected lines can also be divided into three groups on the basis of their excitation potentials, with 4 low excitation Fe I lines ($\chi_e < 2.5$ eV), 4 high excitation Fe I lines ($\chi_e > 4$ eV) and 2 Fe II lines. Each group of lines has a different sensitivity to temperature. All the lines within a given group have nearly the same temperature sensitivity, since they have, firstly, nearly the same excitation potential and, secondly, relatively similar line strengths in the solar spectrum. We paid attention to the fact that lines with low and with high Zeeman sensitivity were present in each excitation potential group, although unblended Fe II lines with large Landé factors are notoriously rare. The Fe II 6149 Å line, however, has (at least for spatially resolved fields, which is not the case here) the Zeeman sensitivity usually associated with twice its Landé factor due to its peculiar splitting pattern – its π-components lie at the same wavelengths as its σ-components – (cf. Mathys 1990; Lites 1993). Although not ideal for our purposes (since we do not resolve the magnetic features) this is the most Zeeman sensitive Fe II line in our spectra. Due to the different temperature responses of the low and high excitation lines, their combination can, in principle, constrain the temperature difference between the magnetic and non-magnetic component.

Although the observed data spreads over a very large spectral range, we restrict ourselves to lines lying between 6000 Å and the atmospheric cutoff at 6806.7 Å in order to minimize the wavelength dependence of the atmospheric models (e.g. wavelength dependence of limb darkening, continuum opacity, etc.). The value of the macroturbulence was required to be unique for all the lines belonging to one group, but could vary from one group to another. The three values for the macroturbulence we get, one for each of the Fe I groups (low/high excitation) and one for the Fe II group, did not differ significantly from one another. The values we cite in the following are the averages over these 3 values.

4. Fundamental stellar parameters

To ensure maximum accuracy of the magnetic field measurements, we carried out a "preanalysis" consisting of the determination of typical stellar parameters such as the effective stellar temperature, T_{eff}, the rotational velocity, $v \sin i$, the iron abundance, Fe/H, the gravitational acceleration, g, and the microturbulence, v_{mic}. All these parameters were determined using the same inversion code and models as used for the following magnetic analysis. Since our line sample contains lines with different temperature sensitivities (different excitation potentials and ionization stages), we are able to determine accurate T_{eff} values for our stars.

4.1. Solar fits

We first carried out fits to the solar integrated flux spectrum of Neckel (1994), i.e. the spectrum of the sun observed "as a star". Since all the fundamental parameters of the sun we are interested in are very well known, we can fine-tune those atomic parameters we wish to keep fixed during the subsequent determination of stellar fundamental quantities. Using the solar effective temperature, T_{eff} = 5780 K, a logarithmic iron abundance of 7.5 (on a scale on which the H abundance amounts to 12.0) and the logarithm of the gravitational constant $\log g$ = 4.5 with the solar $\log gf$ values tabulated by Thévenin (1990) we obtained a fit that did not satisfy our expectations. Consequently, we redetermined the $\log gf$ values from a fit to the spectrum of Neckel (1994). The difference between the Thévenin values and those obtained here may be due to differences between the temperature structure of the atmospheric models used by him and the one used by us, to differences between the used macroturbulence profile shape, to difference in the way the Van der Waals broadening is treated, or to the finite number of angles on the stellar disc at which we compute the line profiles. The $\log gf$ values derived by us using a standard solar Fe abundance of 7.50 (Holweger et al. 1990; Johansson et al. 1994), even if they were to be incorrect in an absolute sense, are best suited to our analysis. Indeed, they should give the most accurate values of stellar fundamental parameters relative to the sun, since our code, the model atmospheres etc. have been calibrated using the sun. The other parameters, such as the rotational velocity and the microturbulence, which were also outputs of the fitting procedure, have typical solar values ($v \sin i$ = 1.96 km s^{-1}, v_{mac} = 3.4 km s^{-1}, v_{mic} = 1.0 km s^{-1}).

The $\log gf$ values of Thévenin (1990) are listed in the 6th column of Table 3, while those resulting from our fit, and which were later used to determine the fundamental parameters of the other stars, are listed in the last column.

4.2. Stellar fits

The free parameters of the inversion of the stellar spectra were the effective temperature, the iron abundance, the rotational velocity, the micro- and macroturbulence, and the gravitational acceleration. The values obtained from these fits are listed in

Table 4. The structure of this table is identical to that of Table 2, except that an additional column with the derived microturbulence, v_{mic}, has been added at its end. The stellar parameters we obtain are on the whole compatible with the literature values shown in Table 2. Some discrepancies can be found, but they lie within a reasonable range. Our "macroturbulent velocities" are generally larger than those found in earlier analyses (Table 2), mainly because the v_{mac} values listed in Table 4 contain a substantial, but unknown contribution from the instrumental profile for reasons described in Sect. 3. Also, since we have avoided using too strong lines, it is difficult to distinguish between micro- and macroturbulence. Our microturbulence values may thus be systematically too small and are compensated by too large macroturbulence values though they are in reasonable agreement with those compiled by Gray (1988) and those determined by Valenti (1994).

We now briefly discuss some of the tabulated parameters. First, for HR 2667 ours are the first measurements of $v \sin i$ and v_{mac}. Secondly, the most discrepant parameter besides v_{mac} is $\log g$. For 5 stars we find $\log g$ values which differ by more than 0.2 from literature values, although for 2 of these stars only a single previous $\log g$ determination is known to us (HR 2667 and HR 4979). One reason for this discrepancy could be that we do not have any strong lines with prominent damping wings, the classical diagnostic for $\log g$, in our sample. On the other hand we have carried out a number of calculations with the widely used Ca I 6162 Å line and have found that it does not provide more accurate $\log g$ values than the line sample used by us, since its damping wings are just as sensitive to other stellar atmospheric parameters, so that combinations of other parameters can easily mask an incorrect g value. The remaining parameters agree on the whole very well with literature values.

The star showing the largest difference between our and previous analysis is α Cen B. Our temperature lies $\approx$ 130 K above and our abundance $\log$ [Fe/H] $\approx$ 0.2 dex below previous determinations. To a certain extent temperature and abundance can compensate each other, so that we cannot rule out that such an effect could have influenced our results.

5. Magnetic field analysis of ϵ Eri

In this section, we describe tests carried out on our spectra of ϵ Eri, the late-type star for which the literature on magnetic investigations is the most abundant. During all the following analysis, the values of the temperature of the non-magnetic component, T_{n-mag}, the gravitational acceleration, g, the microturbulence velocity, v_{mic} and the iron abundance were set to the values determined in the stellar parameter analysis of Sect. 4.2. Following the reasoning given in Sect. 3 the $\log gf$ values are now free parameters of the fitting procedure. Depending on the specific goal of each test, the remaining parameters of the analysis (v_{mac}, the magnetic field strength B, the filling factor α and the effective temperature of the magnetic region T_{mag}) were individually left free or kept fixed.

5.1. Is there a measurable magnetic field on ϵ Eri?

First the magnetic sensitivity of a line pair was analyzed. We assumed $T_{mag} = T_{n-mag}$ and tested, using two different methods, if a magnetic field could be detected at all in our ϵ Eri spectra. The line pair used consists of the low-g ($g_{eff} = 1.0$) Fe I 6240.6 Å line and of the high-g ($g = 2.5$) Fe I 6173.3 Å line, a standard pair often used for stellar magnetic field measurements (e.g. Marcy 1984, Saar 1988). These two lines have the same excitation potential ($\chi_e = 2.22$ eV) and nearly the same strength, so that their reaction to temperature variations should be similar.

The method commonly used with radiative transfer calculations to determine the magnetic parameters (i.e. magnetic field strength and filling factor) consists of first fitting a low-g line without a magnetic field in order to determine the macroturbulent velocity, v_{mac}. Then, in a second step the magnetically sensitive line is fitted employing the v_{mac} obtained in the first step, which yields the magnetic parameters of the star. We refer to this method as the *consecutive fitting procedure*. We first illustrate this method under the assumption that the star has no magnetic field. Fig. 1a shows the fit obtained with no magnetic field, i.e. the low-g line has been fitted alone and the parameter v_{mac} of this fit was taken to calculate the high-g line with $B = 0$. In this figure, as well as in the following figures, the solid line represents the observations, while the dashed line is the fit. The dot-dashed curve is the difference between the observations and the fit enhanced by a factor of 10 and shifted by 0.2. The two dotted horizontal lines delineate the 1-σ noise interval, i.e. the interval within which the dot-dashed curve should mainly lie for a good fit to the data. Note the difference in the quality of the fits to the two lines. Whereas the fit errors (dot-dashed curve) for the low-g line lie mainly within the 1-σ error bars of the data, this is not true for the high-g line, where most of the fit errors exceed 1-σ and some are even larger than 3-σ and thus highly significant. Hence a completely field-free model does not reproduce the data well.

Next we repeat the above procedure, but now with the magnetic field strength set to $B = 1500$ G and the filling factor α a free parameter for the fit to the high-g line. The resulting profiles are shown in Fig. 1b. The inversion code returns $\alpha = 0.08$. An improvement in the quality of the fit is clearly seen when a magnetic field is used ($\chi^2 = 1.51$ versus $\chi^2 = 4.75$ for the fit to both lines when $B \equiv 0$).

Now, consider a slightly different procedure for fitting the two lines. We call it the *simultaneous fitting procedure*. As its name suggests, both lines are fitted simultaneously, with the macroturbulence and the magnetic field determined at the same time (only a single value of v_{mac} is derived for both lines since they are members of the same group). Fig. 2a shows the fit obtained in this manner without a magnetic field ($\chi^2 = 2.77$), while Fig. 2b represents a similar fit obtained with a magnetic field ($\chi^2 = 1.44$) whose parameters are $B = 1500$ (fixed) and $\alpha = 0.11$ (free). In this case the improvement achieved with the use of a magnetic field is much smaller than with the consecutive fitting procedure, mainly due to the improved quality of the fit without a magnetic field. Although the fit to the low-g line is

Table 4: Stellar parameters

Name	HR	Spectral Type	T_{eff} [K]	$\log g$	log[Fe/H]	$v \sin i^*$ [km s^{-1}]	v_{mac}^* [km s^{-1}]	v_{mic}^* [km s^{-1}]
58 Eri	1532	G1V	5830	4.6	+0.06	3.2	5.0	1.0
α Cen A	5459	G2V	5750	4.4	+0.18	2.7	4.9	1.0
	2667	G3V	5880	4.5	−0.10	2.3	4.2	1.0
	3538	G3V	5760	4.6	+0.14	1.8	4.1	1.0
	4979	G3V	5710	4.3	+0.20	2.7	5.2	1.1
61 Vir	5019	G6V	5590	4.5	−0.05	2.0	4.4	1.0
τ Ceti	509	G8V	5350	4.5	−0.49	1.1	3.7	1.0
40 Eri A	1325	K1V	5210	4.5	−0.36	0.8	3.9	1.0
α Cen B	5460	K1V	5150	4.5	+0.04	1.2	4.1	0.9
36 Oph B	6401	K1V	5120	4.4	−0.37	1.9	5.1	1.0
ϵ Eri	1084	K2V	5080	4.6	−0.17	1.6	4.3	1.0
	5568	K4V	4630	4.3	−0.21	1.2	4.8	1.0
ϵ Indi	8387	K5V	4680	4.3	−0.31	1.2	5.6	1.0

* See text (Sects. 3 & 4.2) for a discussion of these parameters
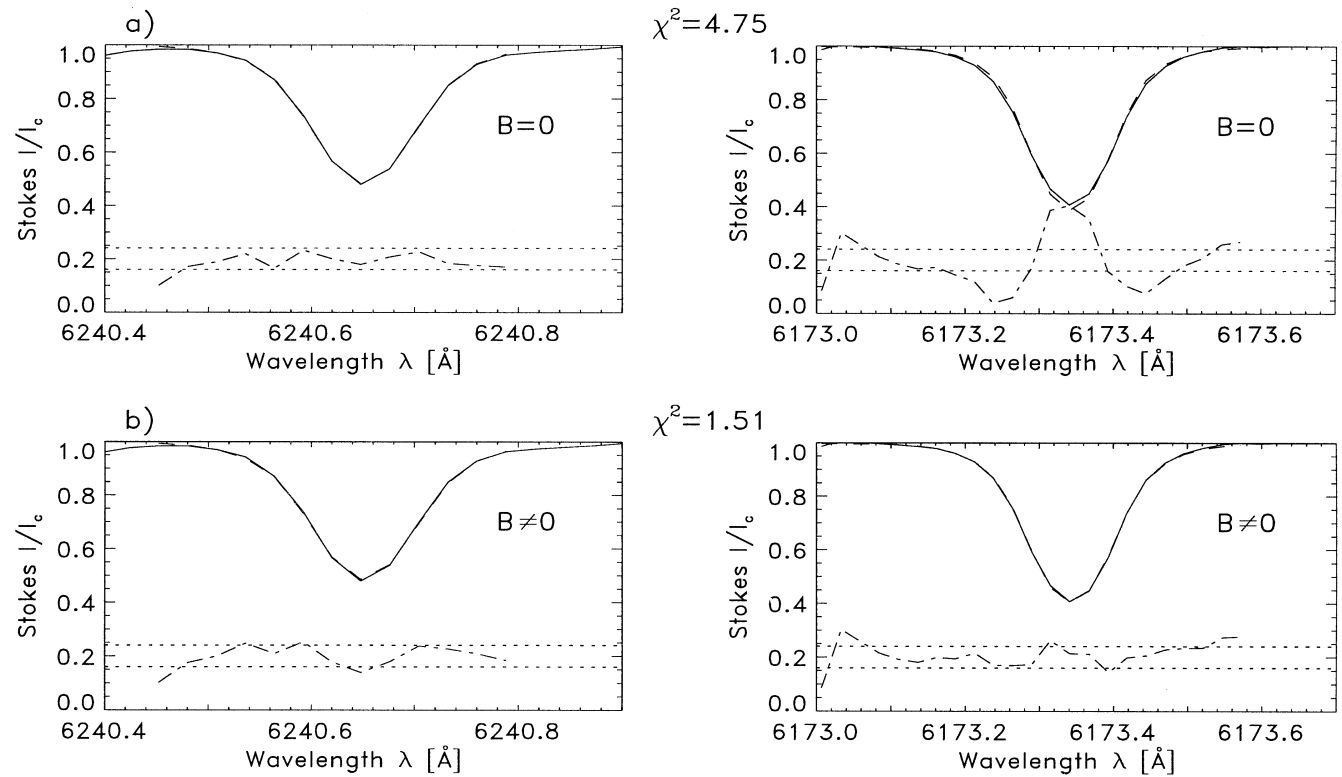
Fig. 1a and b. Fits to a line pair of ϵ Eri with the consecutive fitting procedure. **a** The low-g line (Fe I 6240 Å) was fitted alone and the v_{mac} deduced from this fit was then used to calculate the high-g line (Fe I 6173 Å), with $B = 0$ imposed. Solid curves: observed profiles, dashed curves: synthetized profiles. **b** Same as for Fig. 1a, but the fit to the high-g line was carried out with a fixed magnetic field of strength 1500 G. The free parameter of the fitting procedure was the filling factor. The dot-dashed curve in each frame is the difference between the observed and the synthetic line profile, amplified by a factor of 10 and shifted for clarity. The two dotted lines outline the ± 1-σ level of uncertainty imposed on fits by the noise in the data. Except for the 6173 Å line in the upper right frame all profiles are satisfactorily fitted, in the sense that 65% or more of the difference points lie within the error bars. The reduced χ^2 of the fit to both lines is indicated

now somewhat worse than before, the fit to the high-g line is greatly improved. For no point does the error in the fit reach the 3-σ level. Consequently, the very existence of a magnetic field on ϵ Eri (or other cool stars) is not as obvious as some pre-

vious analyses, carried out using the consecutive fitting procedure, suggested (in a modified manner, including more iteration steps this procedure has been used by, e.g. Basri & Marcy 1988, Marcy & Basri 1989). It also highlights the care that must be
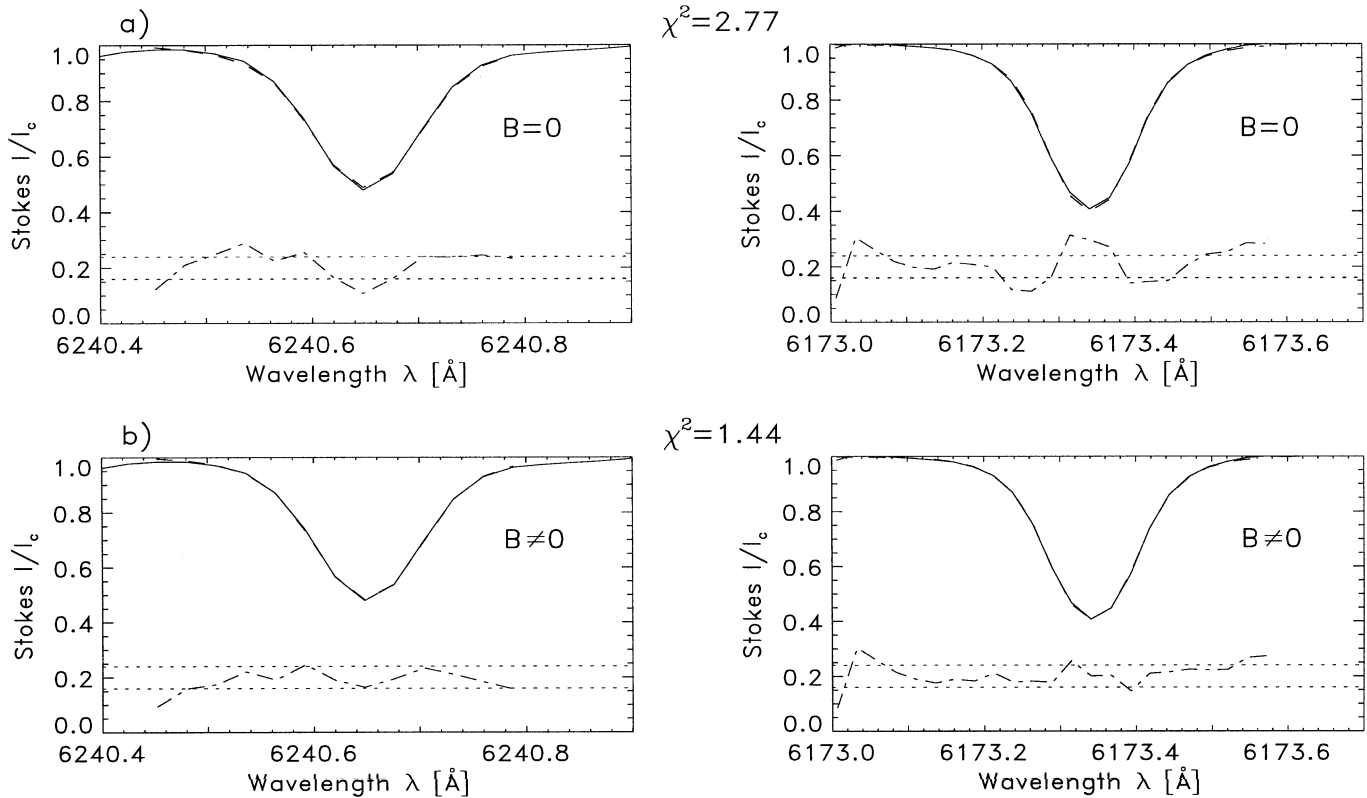
Fig. 2a and b. Simultaneous fit to the same line pair of ϵ Eri as in Fig. 1. **a** Fit with $B = 0$ imposed. **b** Fit with $B = 1500$ G (fixed) and the filling factor and macroturbulence as free parameters. Again the Fe I 6173 Å line does not satisfy the criterion for a good fit if $B = 0$ (see caption of Fig. 1), although only by a small amount this time

accorded to such an analysis. We see no reason why the value of the macroturbulence obtained from the low-g line alone should be better suited for the line pair than a value obtained from a simultaneous fit to both lines including a magnetic component as free parameter.

All the results presented from now on in this paper have been obtained with the simultaneous fitting procedure unless otherwise specified.

5.2. Blending of Fe I 6173 Å and its removal

We noted that if the consecutive fitting procedure is used (see Sect. 5.1) and both the rotational velocity, $v \sin i$ and the macroturbulence are determined during the fit to the low-g_{eff} line and are then kept fixed during the fit to the high-g_{eff} line, very large, unphysical values of the field strength are obtained. This is due to the blends affecting the wings of Fe I 6173 Å. Since no broadening parameters are left free during the fit to the magnetically sensitive line, the inversion code chooses very large values for the magnetic field strength (up to 5000 G) combined with small filling factors to account for the blends situated in the line wings.

Obviously the blending of Fe I 6173 is a major problem for our analysis. We therefore removed these blends in a simple manner. We used the two stars α Cen A and α Cen B, which are well studied, old and show low levels of magnetic activity, as template. We assume these two stars to be free of detectable

magnetic fields. They are of spectral type G2 and K1 respectively and the strengths of their Fe I lines are very different. The best fits without magnetic fields (simultaneous fits to the 10 lines with $B = 0$, i.e. the fits whose resulting parameters are tabulated in Table 3) to these two stars were taken and subtracted from the corresponding observed profiles. We then assumed the blends to be Fe I lines, since these are the most common spectral lines in G and K stars. Their equivalent widths can then be scaled to correspond to those of the other Fe I lines observed in the stellar spectrum to be corrected. For all the other stars, we interpolated between these two resulting "blend-profiles" as a function of the equivalent width of the Fe I 6173 Å line and removed the scaled blend-profiles from the spectra. The resulting Fe I 6173 Å profiles are, as expected, much more symmetric. They do not appear to be overcorrected. Single points may lie above the continuum value, but always within the limits of the noise level, so that we are confident in the reliability of the correction. Note that the results shown in Figs. 1 and 2 and discussed in Sect. 5.1 are already based on the deblended Fe I 6173 Å line.

5.3. Can α and B be determined individually?

As demonstrated in the Sect. 5.1, the χ^2 is reduced when a magnetic field is introduced into fits to the spectra of ϵ Eri.

Given the presence of a magnetic field on ϵ Eri, we want to investigate the reliability of deduced values of the magnetic

field strength and filling factor. For that purpose, two line pairs (pair 1: Fe I 6173 Å and Fe I 6240 Å, $\chi_e = 2.22$; pair 2: Fe I 6820 Å and Fe I 6842 Å, $\chi_e = 4.64$) have been fitted, with both lines of each pair being fitted simultaneously. The magnetic field strength was prescribed, while the filling factor was allowed to vary. Fig. 3 shows the fits to the low χ_e line pair obtained with field strengths of 500 G, 1000 G, 1500 G and 2000 G. The high excitation lines present a very similar picture. It is obvious that no significant differences are observed between these 4 fits, neither in the profiles themselves nor in the difference spectra (dot-dashed curve), or in the reduced χ^2 values. Hence one cannot trust the magnetic field strengths or filling factors derived for ϵ Eri from optical spectra, at least for data of the S/N (> 250) and resolution (10^5) analyzed here. Since relatively few facilities can obtain data of higher spectral resolution than the ESO CAT/CES, our result implies that it is very difficult (at best) to separate α and B on ϵ Eri with optical spectra. The magnetic flux αB, however, is a more reliable parameter. Whereas α and B differ by a factor of 4 in the 4 frames, αB changes by a factor of roughly 1.7. The two line pairs also provided values of the magnetic flux consistent within their uncertainties: 165 ± 30 for pair 1 and 180 ± 45 for pair 2 for $B = 1500$ G. Finally, $\sqrt{\alpha}B$ varies by an even smaller amount, roughly 1.5, in agreement with expectations for incompletely Zeeman split lines (Gray 1984a, Saar 1988). All the published values of magnetic field measurements of moderately active cool stars carried out with optical spectra are affected by the same problem to a greater or lesser degree. The above result is independent of whether blends are removed from Fe I 6173 Å or not (the plotted profiles have been corrected for blends). The flux values quoted in the figure are also based on blend corrected Fe I 6173 Å; without correction, agreement between the computed magnetic fluxes for different values of B, and for different line pairs, is less satisfactory.

When all the lines are fitted simultaneously, allowing different values of the macroturbulence for each group of lines, i.e. Fe I with high excitation potential, Fe I with low excitation potential and Fe II, the flux values obtained are similar to those obtained from each line pair separately.

5.4. Temperature of the magnetic features

It is in principal possible to constrain the temperature of the magnetic features on a stellar surface if the magnetic field can be determined individually from sets of lines with widely different excitation potentials. The basic idea is that if $T_{mag} \neq T_{n-mag}$, then the relative strengths of lines with different χ_e will be different in the magnetic feature compared to their relative strengths in the field-free part of the star. For example, if $T_{mag} > T_{n-mag}$, then the low excitation lines are weakened relative to the high excitation lines in the magnetic features. The relative contribution of the magnetic features will then be smaller in low χ_e lines than in high χ_e features. Thus, if we use $T_{mag} = T_{n-mag}$ when we calculate the synthetic profiles then one may expect two consequences to be observed. Firstly, the metal abundance (or $\log gf$) necessary to produce a good fit of the (weakened)

low excitation lines will be lower than that needed for the high excitation lines. Secondly, the αB values obtained from the low χ_e lines should be smaller than the αB values obtained from the high χ_e lines. Recall that this happens because the strengths of the low excitation lines in the hot magnetic component are reduced compared to their strength in the cooler field-free atmosphere. They will only slightly affect the composite profiles and this will be mistaken with a low magnetic flux if the temperature of the magnetic element during the inversion is assumed to be lower than it actually is. The opposite would be the case for magnetic features cooler than the field-free atmosphere.

In order to test whether our lines are sufficiently sensitive to detect such effects on moderately active stars we used the two line pairs already discussed in Sect. 5.3 and fitted their "deblended" profiles simultaneously for a sequence of T_{mag} values. The temperature of the field-free surroundings was kept at the values tabulated in Table 2, while the temperature of the magnetic feature systematically varied within a range of ± 500 K relative to that of the surroundings. Since the magnetic field value cannot be determined uniquely from the fit alone, we prescribed it to be 1500 G. The quality of the fits (measured by the reduced χ^2) does not change significantly when the temperature of the magnetic features is changed, irrespective of whether we choose values hotter or cooler than the surroundings. The αB values obtained with both line pairs are also always compatible with each other within the tested temperature range. Apparently, the magnetic flux is not sensitive enough to tell alone which temperature is better without considering other parameters. The αB returned by both line pairs, however, are inversely proportional to the temperature of the magnetic region. This behaviour is expected since the continuum intensity is lowered, along with the temperature (the temperature gradients of the Kurucz models with different T_{eff} are rather similar). Thus, in order to have the same influence on the line profiles, a cool magnetic region has to contain a larger magnetic flux.

When we compare the $\log gf$ values obtained with these fits to those obtained with the solar fit a general trend is observed. As the temperature of the magnetic features is lowered the $\log gf$ values returned by the inversion code increase strongly for the low excitation lines and less strongly for the high excitation lines. Within each group, both lines show a consistent behaviour. The differences between the two groups are smallest when the temperature of the magnetic component is similar to or up to 500 K hotter than in the surroundings, suggesting that the temperature of the magnetic component lies within this range. Similar temperature enhancements are seen in the magnetic elements composing solar faculae (see Solanki 1993 for a review), suggesting that the detected magnetic fields on ϵ Eri are facular in nature, in agreement with expectations (e.g. Saar et al. 1986). In the following we assume $T_{mag} \sim T_{n-mag}$, in agreement with the above result and previous measurements of stellar magnetic fields.
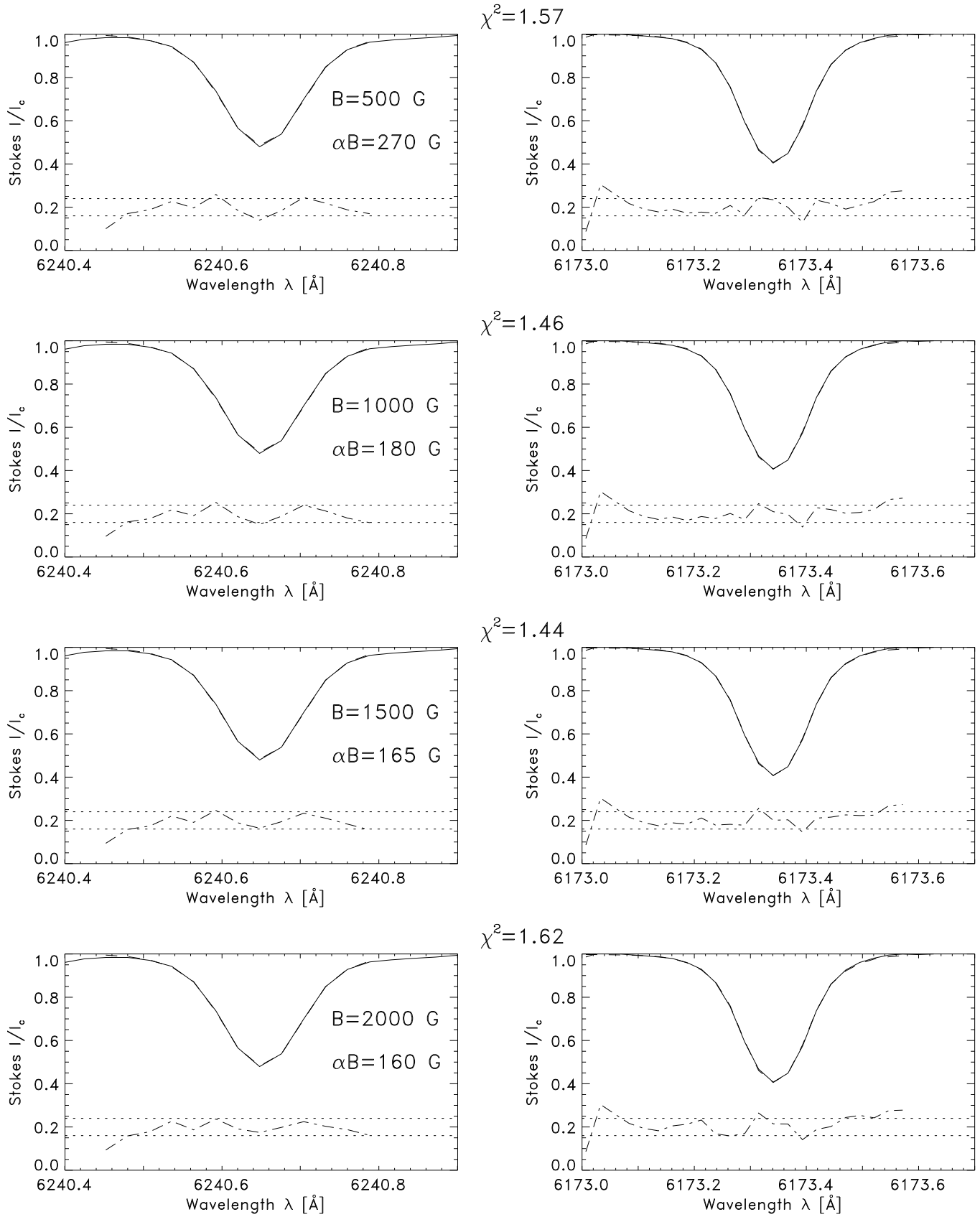
Fig. 3. Simultaneous fit to a line pair of ϵ Eri for various fixed values of the magnetic field strength B. From top to bottom: $B =$ 500 G, 1000 G, 1500 G and 2000 G. Blends in the wings of Fe I 6173 Å have been removed according to the prescription given in Sect. 5.2

Table 5. Magnetic parameters

Name	HR	Spectral Type	$\alpha B_{\text{lo.ex.}}$ [G]	$\alpha B_{\text{hi.ex.}}$ [G]	αB_{all} [G]	P_{rot} [days]	F_x $[F_x\odot]$
58 Eri	1532	G1V	135±60	270±60	330±210	10.8	15.0
α Cen A	5459	G2V	–	225±60		29.0	0.3
	2667	G3V	0	180±60			
	3538	G3V	0	150±45		15.0	5.0
	4979	G3V	0	105±45			1.9
61 Vir	5019	G6V	0	0		32.7	≤ 0.4
τ Ceti	509	G8V	0	60±90		31.9	0.25
40 Eri A	1325	K1V	30±75	90±60	30±60	37.0	1.1
α Cen B	5460	K1V	–	0		43.0	0.6
36 Oph B	6401	K1V	135±30	90±60	60±45	21.1	6.0
ε Eri	1084	K2V	165±30	180±45	165±30	11.7	10.0
	5568	K4V	105±30	225±60	75±30		<0.6
ε Indi	8387	K5V	90±30	Blended			1.6

6. Magnetic field results for the complete stellar sample

We employed the following procedure to measure the magnetic flux values for all stars in our sample. We always used the simultaneous fitting procedure described in Sect. 5.1. First, the two line pairs, 6173 Å/6240 Å and 6820 Å/6842 Å, were each fitted separately. Spectra corrected for the blends of Fe I 6173 Å, as explained in Sect. 5.2, were used. Since none of the stars allowed B to be uniquely separated from α, the magnetic field strength was frozen at 1500 G, while the filling factor was a free parameter. We assumed $T_{\text{mag}} = T_{\text{n-mag}} = T_{\text{eff}}$, whereby the values of T_{eff} determined in Sect. 4.2 was employed. If both line pairs gave a flux value larger than the uncertainties, a simultaneous fit to all 10 lines listed in Table 3 was performed.

Table 5 gives magnetic fluxes resulting from the fits to the low excitation line pair (listed under the heading $\alpha B_{\text{lo.ex.}}$), the high excitation line pair ($\alpha B_{\text{hi.ex.}}$) and all 10 lines (αB_{all}) together with their 1-σ uncertainties.

We require all 3 tabulated αB values to be above the uncertainty and of similar magnitude in order to accept the detection of the magnetic field as unambiguous. In this sense ϵ Eri is the only star in our sample which unambiguously shows a magnetic field, while 58 Eri, 36 Oph B, and HR 5568 show evidence of varying reliability of a magnetic field. ϵ Indi is another possible, but less secure candidate. The rest of the stars do not exhibit any sign of a magnetic field. Our data suggest that $\alpha B \lesssim 100$ G on these stars.

We also observe a number of other effects from Table 5. Thus, for example, there may well be a residual blending problem. Thus the high excitation lines return larger αB values for all stars earlier than G6 or later than K2, including stars which are known to be extremely inactive (α Cen A fits in with the other early G stars in this respect). In ϵ Indi these lines are visibly distorted by blends, which suggests that they might be similarly affected for HR 5568. Saar (1987) has demonstrated strikingly how much more cluttered the spectrum becomes from early to mid K stars. Hence for the two coolest stars in the sample the result from the low excitation lines must be treated with caution

as well, since our blend removal scheme based on the K1 dwarf α Cen B may no longer be adequate.

The αB values derived from the low excitation lines on 58 Eri, ϵ Eri and 36 Oph B, in contrast, are more likely to be reliable and we consider them to be the only reasonably reliable magnetic candidates in our list. They are also the 3 stars with the strongest X-ray emission.

A careful analysis of these stars in the infrared spectral range may be able to detect more certain signs of a magnetic field due to the higher magnetic sensitivity and the lower line density (reducing the problem of blends) in the infrared spectrum. Even then, in order to obtain the best results, fits to the low and high g_{eff} lines should be performed simultaneously with α, B and v_{mac} as free parameters. The magnetic flux values which we obtain for ϵ Eri and 40 Eri A (the only two stars common to both investigations) are consistent with those obtained by Valenti et al. (1995) from 1.5 μm spectra. Note that these values are much lower than those cited in earlier analyses carried out with optical spectra (see Saar 1990 and Valenti et al. 1995). The reason for the discrepancy between our and earlier results (e.g. Marcy 1984, Basri & Marcy 1988, Mathys & Solanki 1989, Marcy & Basri 1989) lies in the different analysis strategy.

The simultaneous fit to 10 lines does not tend to produce lower formal uncertainties in the magnetic flux values. All the same it is important to use more than one line pair in order to minimize the effects produced by weak undetected blends. A larger number of line pairs also ensures a better magnetic sensitivity. In particular, the magnetic field contribution to weak lines, like the high excitation line pair (Fe I 6820 Å and Fe I 6842 Å) used in this work, is more likely to be hidden by noise, etc., than in the case of the deeper profiles, such as those of the low-excitation line pair (Fe I 6173 Å and Fe I 6240 Å). Finally, such fits provide another consistency check on the results.

7. Conclusions

We have carried out a thorough analysis of high resolution, high signal-to-noise Echelle spectra covering a large wavelength

range of 13 relatively bright, inactive to moderately active late-type dwarfs using an inversion code which simultaneously determines the stellar parameters of interest. After determining the fundamental parameters of the stars (T_{eff}, $\log g$, [Fe/H], $v \sin i$, v_{mic}), we carried out a search for magnetic fields on them. Particular attention was paid to the relatively active star ϵ Eri (K2V), the late-type star whose magnetic field has been measured most often. This star was used to compare two fitting procedures and to test various assumptions. Later we applied our inversion procedure to the 12 remaining stars in our sample. The large spectral range of the data allowed us to use carefully selected groups of lines, which also permitted us to test the internal consistency of our results.

The magnetic flux αB can be reliably determined, but we were unable to separate α from B and expect this to be a problem in general for moderately active solar-type stars, at least with optical data with spectral resolution $\leq 10^5$ and S/N ≤ 250.

The determination of the temperature of the magnetic features is also a difficult undertaking. Nevertheless, we developed a technique which, when applied to ϵ Eri indicated that the temperature in the *detected* magnetic features is higher (by 0-500 K) than in the field-free atmosphere. As has been argued by Saar et al. (1986), Basri et al. (1990) and Saar & Solanki (1996) the magnetic signature of cool structures, such as starspots, are not expected to be detected in visible spectra.

The good agreement between our results and those of Valenti et al. (1995) – probably the two most careful searches for magnetic fields on moderately active stars – gives us confidence that it is possible to determine fields on such stars with an accuracy of roughly 100 G in αB. As already pointed out by numerous previous authors (e.g. Gray 1984a, Saar 1988) the best determined quantity is $\sqrt{\alpha}B$, at least for optically thin lines in the visible, although the average field strength αB is almost equally well determined. Most of the analyses carried out to date, at least those not based on radiative transfer, probably gave too high values of the magnetic flux on moderatively active stars. In our sample, we believe an unambiguous determination of magnetic flux can be claimed only for ϵ Eri. Three other stars show evidence of a magnetic field but have less reliably determined fluxes. Of these three stars we consider 58 Eri and 36 Oph B to be probable detections, while the results for the K4 dwarf HR 5568 must be considered with caution due to possible blending of the spectral lines. The remaining stars have no detectable line profile distortions that could be assigned with confidence to a magnetic field. We expect the spatially averaged field strength on these stars to lie below 100 G.

Finally, our analysis confirms once more that the presence of small blends can have a disastrous influence on the magnetic parameters obtained when fitting one pair of lines (cf. Gondoin et al. 1985, Saar et al. 1986, Saar 1988). Careful deblending of lines and/or use of multiple line pairs helps reduce this problem. Indeed, we find that if only a single line pair is employed the number of stars with seeming magnetic detections is much larger than if one requires, as we do, that two different sets of lines give similar values of the magnetic parameters.

References

Abia C., Rebolo R., Beckman J.E., Crivellari L., 1988, A&A 206, 100
Anderson H., Edvardsson B., 1994, A&A 290, 590
Ayres T.R., Fleming T.A., Simon T. et al., 1995, ApJS 96, 223
Baliunas S.L., Donahue R.A., Soon W.H. et al., 1995, ApJ 438, 269
Basri G.S., Marcy G.W., 1988, ApJ 330, 274
Basri G.S., Marcy G.W., 1994, ApJ 431, 844
Basri G., Marcy G.W., Valenti J.A., 1990, ApJ 360, 650
Basri G., Marcy G.W., Valenti J.A., 1992, ApJ 390, 622
Bell R.A., Edvardsson B., Gustafsson B., 1985, MNRAS 212, 497
Blackwell D.E., Lynas-Gray A.E., 1994, A&A 282, 899
Bruning D.H., 1984, Ph.D. thesis, Univ. New Mexico
Cayrel de Strobel G., Bentolila C., 1989, A&A 211, 324
Cayrel de Strobel G., Hauck B., François P. et al. 1992, A&AS 95, 273
Char S., Foing B.H., Beckman J., Garcia López R.J., Rebolo R., 1993, A&A 276, 78
Chmielewski Y., Cayrel de Strobel G., Lebreton Y., Bentolila C., 1991, A&A 247, 368
Chmielewski Y., Friel E., Cayrel de Strobel G., 1992, A&A 263, 219
Donahue R.A., Saar S.H., Baliunas S.L., 1996, ApJ 466, 384
Donati J.-F., Semel M., Rees D.E., Taylor K., Robinson R.D., 1990, A&A 232, L1
Donati J.-F., Semel M., Rees D.E.,1992a, A&A 265, 669
Donati J.-F., Brown S.F., Semel M. et al. 1992b, A&A 265, 682
Dravins D., Nordlund A., 1990, A&A 228, 203
Duncan D.K., 1981, ApJ 248, 651
Frey G.J., Grim B., Hall D.S. et al. 1991, AJ 102, 1813
Gehren T., 1981, A&A 100, 97
Gondoin P., Giampapa M.S., Bookbinder J.A., 1985, ApJ 297, 710
Gray D.F., 1984a, ApJ 277, 640
Gray D.F., 1984b, ApJ 281, 719
Gray D.F., 1988, Lectures on Spectral-Line Analysis: F, G, and K Stars, The Publisher, Arva, Ontario
Gray D.F., 1994, PASP 106, 1248
Gray D.F., Johanson H.L., 1991, PASP 103, 439
Gray D.F., Baliunas S.L., 1994, ApJ 427, 1042
Gray D.F., Baliunas S.L., 1995, ApJ 441,436
Hale A., 1994, ApJ 107, 306
Hallam K.L., Aliner B., Endal A.S., 1991, ApJ 372, 610
Hearnshaw H.B., 1976, A&A 51, 85
Hempelmann A., Schmitt J.H.M.M., Schultz M., Rüdiger G., Stepien K., 1995, A&A 294, 515
Hempelmann A., Schmitt J.H.M.M., Stepien K., 1996, A&A 305,284
Holweger H., Heise C., Kock M., 1990, A&A 232, 510
Johansson S., Nave G., Geller M. et al. 1994, ApJ 429, 419
Kurucz R.L., 1991, in: Precision Photometry: Astrophysics of the Galaxy, A.G. Davis Philip, A.R. Upgren, K.A. Janes (Eds.), L. Davis Press, Schenectady
Lites B.W., 1993, Solar Phys. 143, 229
Marcy G.W., 1984, ApJ 276, 286
Marcy G.W., Basri G., 1989, ApJ 345, 480
Mathys G., 1990, A&A 232, 151
Mathys G., Solanki S.K., 1989, A&A 208, 189

Neckel H., 1994, in: The Sun as a Variable Star: Solar and Stellar Irradiance Variations, J. Pap, C. Fröhlich, H.S. Hudson, S.K. Solanki (Eds.), Cambridge University Press, Cambridge, IAU Coll. 143, 37

Noels A., Grevesse N., Magain P., Neuforge C., Baglin A., Lebreton Y., 1991, A&A 247, 91

Noyes R.W., Hartmann L.W., Baliunas S.L., Duncan D.K., Vaughan A.H., 1984, ApJ 279, 763

Pasquini L., 1992, A&A 266, 347

Pasquini L., Pallavicini R., 1991, A&A 251, 199

Pasquini L., Liu Q., Pallavicini R., 1994, A&A 287, 191

Pierce A.K., Breckinridge J.B., 1973, *KPNO Contr. 559*

Perrin M.N., Cayrel de Strobel G., Dennefeld M., 1988, A&A 191, 237

Queloz D., Babel J., Mayor M., 1995, in: Cool Stars, Stellar Systems and the Sun, IX, R. Pallavicini (Ed.), in press

Randich S., Gratton R., Pallavicini R., 1993, A&A 253, 185

Rebolo R., Crivellari L., Castelli F., Foing B., Beckman J.E., 1986, A&A 166, 195

Rees D.E., Murphy G.A., Durrant C.J., 1989, ApJ 339, 1093

Robinson R.D., 1980, ApJ 239, 961

Robinson R.D., Worden S.P., Harvey J.W., 1980, ApJ 236, L155

Saar S.H., 1987, in: Cool Stars, Stellar Systems and the Sun. V, J.L. Linsky, R.E. Stencel (Eds.), Springer, New York, p. 10

Saar S.H., 1988, ApJ 324, 441

Saar S.H., 1990, in: Solar Photosphere: Structure, Convection and Magnetic Fields, J.O. Stenflo (Ed.), Kluwer, Dordrecht, IAU Symp. 138, 427

Saar S.H., 1994, in: Cool Stars, Stellar Systems and the Sun, VIII, J.-P. Caillault (Ed.), Astron. Soc. Pacific Conf. Ser., Vol. 64, p. 319

Saar S.H., 1996, in: Stellar Surface Structure, K.G. Strassmeier, J.L. Linsky (Eds.), Kluwer, Dordrecht, IAU Symp. 176, 237

Saar S.H., Linsky J.L., 1985, ApJ 299, L47

Saar S.H., Osten R.A., 1996, MNRAS in press

Saar S.H., Solanki S.K., 1997, A&A , in press

Saar S.H., Linsky J.L., Beckers J.M., 1986, ApJ 302, 777

Saar S.H., Linsky J.L., Duncan D.K., 1986, in: Cool Stars Stellar Systems and the Sun, IV, M. Zeilik, D.M. Gibson (Eds.), Springer Verlag, New York, p. 275

Schrijver C.J., 1983, A&A 127, 289

Simmons G.J., Blackwell D.E., 1982, A&A 112, 209

Smith M.A., 1983, PASP 95, 268

Soderblom D.R., 1985, PASP 97, 54

Solanki S.K., 1987, Ph.D. Thesis, No. 8309, ETH, Zürich

Solanki S.K., 1992, in: Cool Stars, Stellar Systems and the Sun, VII, M.S. Giampapa, J.A. Bookbinder (Eds.), Astron. Soc. Pacific Conf. Ser., Vol. 26, p. 211

Solanki S.K., 1993, Space Sci. Rev. 61, 1

Solanki S.K., Rüedi I., Livingston W., 1992, A&A 263, 339

Solanki S.K., Montavon C.A.P., Livingston W., 1994, A&A 283, 221

Steenbock W., 1983, A&A 126, 325

Stenflo J.O., Lindegren L., 1977, A&A 59, 367

Strassmeier K.G., Rice J.B., Wehlau W.H. et al. 1991, A&A 247, 130

Taylor B.J., 1994, PASP 106, 452

Thévenin F., 1990, A&AS 82. 179

Valenti J.A., 1994, Ph.D. thesis, University of California, Berkeley

Valenti J.A., Marcy G.W., Basri G., 1995, ApJ 439, 939

Vogt S.S., Penrod G.D., 1983, PASP 95, 565

Wood B.E., Brown A., Linsky J.L. et al. 1994, ApJS 93, 287